City-Scale Dark Fiber DAS Measurements of Infrastructure Use During the COVID-19 Pandemic

Nathaniel J. Lindsey[1] , Siyuan Yuan[1], Ariel Lellouch[1] , Lucia Gualtieri[1] , Thomas Lecocq[2] , and Biondo Biondi[1]

[1]Geophysics Department, Stanford University, Stanford, CA, USA, [2]Seismology and Gravimetry Department, Royal Observatory of Belgium, Brussels, Belgium

Abstract Throughout the recent COVID-19 pandemic, real-time measurements about shifting use of roads, hospitals, grocery stores, and other public infrastructure became vital for government decision makers. Mobile phone locations are increasingly assimilated for this purpose, but an alternative, unexplored, natively anonymous, absolute method would be to use geophysical sensing to directly measure public infrastructure usage. In this paper, we demonstrate how fiber-optic distributed acoustic sensing (DAS) connected to a telecommunication cable beneath Palo Alto, CA, successfully monitored traffic over a 2-month period, including major reductions associated with COVID-19 response. Continuous DAS recordings of over 450,000 individual vehicles were analyzed using an automatic template-matching detection algorithm based on roadbed strain. In one commuter sector, we found a 50% decrease in vehicles immediately following the order, but near Stanford Hospital, the traffic persisted. The DAS measurements correlate with mobile phone locations and urban seismic noise levels, suggesting geophysics would complement future digital city sensing systems.

1. Introduction

During the recent global coronavirus disease pandemic that began at the end of 2019 (COVID-19), human movement in public spaces became a public health issue as government officials advised or required citizens adopt practices of shelter-in-place, social distancing, and other behavioral interventions to mitigate the spread of the novel coronavirus (Ferguson et al., 2020; Tian et al., 2020). In California, nearly 40 million individuals were ordered to stay indoors by state officials beginning 19 March 2020, except as needed to maintain critical infrastructure operations, conduct essential services, and obtain food or personal exercise. In the San Francisco Bay Area, the order came from city and county officials 3 days earlier on 16 March 2020.

During public health emergencies of this magnitude, measuring human activity and how public spaces are being used becomes critical for many reasons throughout all phase of the pandemic. Monitoring activity levels during early stages of a pandemic can provide scope of contact tracing and containment efforts. During quarantine, quantifying public activity feeds back the required information to public health and government officials to make informed decisions such as if the population is properly following quarantine orders (Oliver et al., 2020; Tizzoni et al., 2014; Wesolowski et al., 2012). Historically, this information has been captured in the months or years following the crisis through in-person surveys, but in the past decade, public and private mobile phone data have become a tool to understand where, when, and how phases of a particular crisis are unfolding in real time. During the COVID-19 crisis, Apple and Google released aggregated mobile phone location services reports beginning 4 April that summarized public infrastructure usage on a county or regional basis (Apple, 2020; Google, 2020). In the San Francisco Bay Area, these reports signaled that vehicle traffic and in-store purchases dropped by 60%–80% in the days following the shelter-in-place order, while grocery and pharmacy visits decreased by 20%. Inferences drawn from mobile phone data appear potentially biased by socioeconomic class, age, and region, but studies have shown that with even less than 10% of users activating location services, aggregated sampling is surprisingly robust (Wesolowski et al., 2013). Nonetheless, to any decision maker, the mobile phone data of a city are segmented by platform, thus requiring the concatenation of multiple, heterogeneous databases before one can understand how, for example, shelter-in-place order impacts are affecting a particular sector of a city. Most importantly, while

pseudo-anonymization and aggregation algorithms are applied to separate the mobile phone user from their urban footsteps, users are likely to still be wary of the causal linkage established by monitoring their passively generated mobile phone data.

An alternative, fully anonymous, absolute signal of city-scale human activity is ever present in the low-level seismic wavefield produced by humans, often called the anthropogenic seismic background. For over two decades, seismologists have referred to these 0.5–50 Hz vibrations as "anthropogenic noise" because they commonly obscure earthquakes and other natural Earth signals (Meremonte et al., 1996). This "noise" is actually composed of seismic waves excited by a multifarious number of moving sources, including vehicles, trucks and trains, buildings and bridges excited by the wind, and generators, pumps, and other motorized systems. Instrumenting an urban area with a few precise inertial seismometers has documented the strong spatial and temporal variabilities associated with the anthropogenic seismic wavefield, from high ground motion amplitudes during the daytime to low ground motion amplitudes during night, weekend, and holiday times; ground motions have even been documented from crowds during sporting matches and between sets of a rock concert (Díaz et al., 2017; Vidale, 2011).

Recently, during the COVID-19 pandemic, recordings from over 95 urban seismometers were studied in a worldwide effort to measure how the quarantine affected anthropogenic seismic wavefield (Lecocq, 2020; Lecocq et al., 2020; Xiao et al., 2020, Poli et al., 2020) with results showing anthropogenic ground motion reductions from 10% to more than 25 100% relative to prequarantine levels measured in average dB around 5-40 Hz. Seismic energy generated by anthropogenic sources propagates mostly as surface waves in all directions. Due to the highly dissipative nature of the near surface, these waves also undergo severe anelastic attenuation, which is exponential with frequency. Therefore, conventional seismometers deployed in cities can only produce low-resolution maps of general human activity levels, biased towards sources close to the stations. Densifying the recording array using thousands of seismometers with sensor separations of 100 m can measure general urban infrastructure usage patterns across a city such as greater noise near commute infrastructure for a period of several months (Inbal et al., 2015). However, the cost to deploy and maintain thousands of independent stations each with its own sensor, data logger, and power supply throughout a city is impractical for even a brief experiment and inconceivable over years.

Distributed acoustic sensing (DAS) is an emerging geophysical method that turns optical fibers into dense seismic recording arrays with virtual receiver points spaced every 1–10 m along the fiber. A DAS experiment consists of connecting an optoelectronic DAS instrument to one end of a standard telecommunications-grade optical fiber. The DAS instrument sends short laser pulses into the optical fiber and measures the subtle phase shifts of Rayleigh scattered light returning to the detector at a predicted two-way travel time (Masoudi & Newson, 2016; Posey, 2000). In this way, the strain field acting on the fiber coupled to the Earth can be sampled at a meter-scale spatial resolution over tens of linear fiber kilometers. Recently, it was shown that DAS can take advantage of otherwise dark telecommunication fibers (Ajo-Franklin et al., 2019; Jousset et al., 2018; Martin et al., 2017) or even be used in combination with lit fiber networks (Wellbrock et al., 2019), effectively leveraging portions of the used or unused modern utility grid for geophysical sensing. In the dark fiber case, DAS recordings commonly capture 10,000–20,000 horizontal fiber-oriented components of the strain field in a time continuous fashion, a scale of seismic acquisition that is not possible with traditional seismometers. An additional advantage for dark fiber DAS is that the instruments are deployed in secure telecommunications utility buildings and the fiber is secure under the road. Therefore, this type of experiment can be rapidly deployed in a few hours and continue to record for years without major operations costs. In urban areas, DAS measurements have already been used for near surface geological imaging (Dou et al., 2017; Fang et al., 2020; Martin, 2018; Spica et al., 2020) and earthquake recording (Lindsey et al., 2017; Martins et al., 2019).

In this paper, we use continuous dark fiber DAS recordings from a telecommunication cable running through Palo Alto, CA, leased from Stanford University IT Services to measure how different public sectors of the city responded to the COVID-19 pandemic quarantine order. We begin by illustrating the diversity of urban soundscapes and the related challenges of disentangling urban ground noise source processes. Then, we show how the broadband nature of DAS buried beside roads in a city captures both high frequency (3–30 Hz) anthropogenic surface waves radiated by vehicles as well as a more interpretable quasi-static or geodetic signal created by the response of the roadbed to point-load vehicle movements,
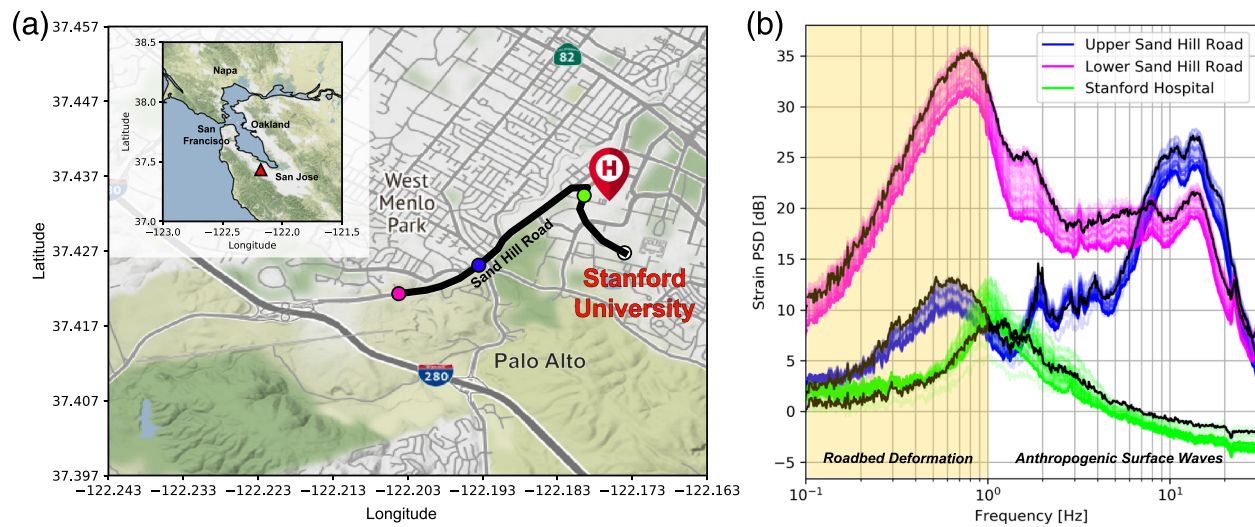
Figure 1. Stanford DAS-2 experiment Array and anthropogenic noise spectra. (a) Map of optical fiber path used for DAS (black line) located in Palo Alto, California (inset, red triangle). Circles color-code a few DAS channels used for detailed analysis (white = quiet reference; green = near Stanford hospital; blue = upper Sand Hill Road; magenta = lower Sand Hill Road). (b) Daily median power spectral density (PSD) of strain data computed for DAS channels shown in (a) highlight strong spatial variability in anthropogenic ground motion, and how this ground motion changed during quarantine. Black curves represent PSD on 01 March 2020. Transparent colored curves fade to solid with increasing experiment date through end of April 2020 (magenta and blue both decrease; green does not show a clear trend). Yellow shading highlights frequency band used to identify vehicles with DAS based on their geodetic roadbed deformation.

specifically the loading and unloading of the road near the fiber. This roadbed deformation signal occurs in a lower frequency range (<1 Hz). We use the geodetic signals to automatically detect individual vehicles and measure their speed, size, and direction on the road. We compare the number of vehicles passing through portions of the public infrastructure around Palo Alto recorded by DAS to aggregated mobile phone location services data and discuss the complementarity of this anonymous geophysical data source.

2. Results

2.1. Exploratory Data Analysis

Over 14.5 TB of continuous DAS strain, data were recorded between 01 March 2020 and 01 May 2020 on the Palo Alto DAS array (see map in Figure 1a). The general characteristics of the local urban seismic background were documented for a subset of DAS channels near Stanford Hospital and Sand Hill Road by computing daily power spectral density (PSD) after some basic preprocessing (see Text S1 in the supporting information). Most DAS channels were dominated by broad frequency maxima spanning half an octave or more (Figure 1b), but the exact frequency peak varied significantly across the array, even within 100 m. A first-order difference is that Sand Hill Road PSD curves were 20–30 dB higher than the non-Sand Hill Road segment. Some channels, like from Upper Sand Hill, also showed minor, narrow frequency peaks. Characteristics of high frequency seismic noise at any one location could be related to varying road features (road turn, stop sign, stop light), nontransportation seismic sources such as building resonance, hydrological pumps or mechanical motors (Coward et al., 2005), soil thickness, and seismic velocity in the upper 30 m (Dou et al., 2017; Nakamura, 1989), the coupling condition of the fiber sensor at that position in the array (Ajo-Franklin et al., 2019). Significant PSD reductions of up to 7 dB were observed at most channels beginning after the first week in March (black traces) to the last day (solid color; transparency decreases with time) in Figure 2b (analyzed in greater detail below). Other channels, including those near Stanford Hospital, showed only one lower frequency peak that did not systematically change during quarantine.

Combining DAS density with multikilometer lateral apertures permitted more targeted exploration of the sources responsible for the urban seismic background. For example, Figure 2a documents vehicles driving at ~15 m/s (33.55 mph) on Sand Hill Road, where the speed limit is 15.65 m/s (35 mph). The data in this
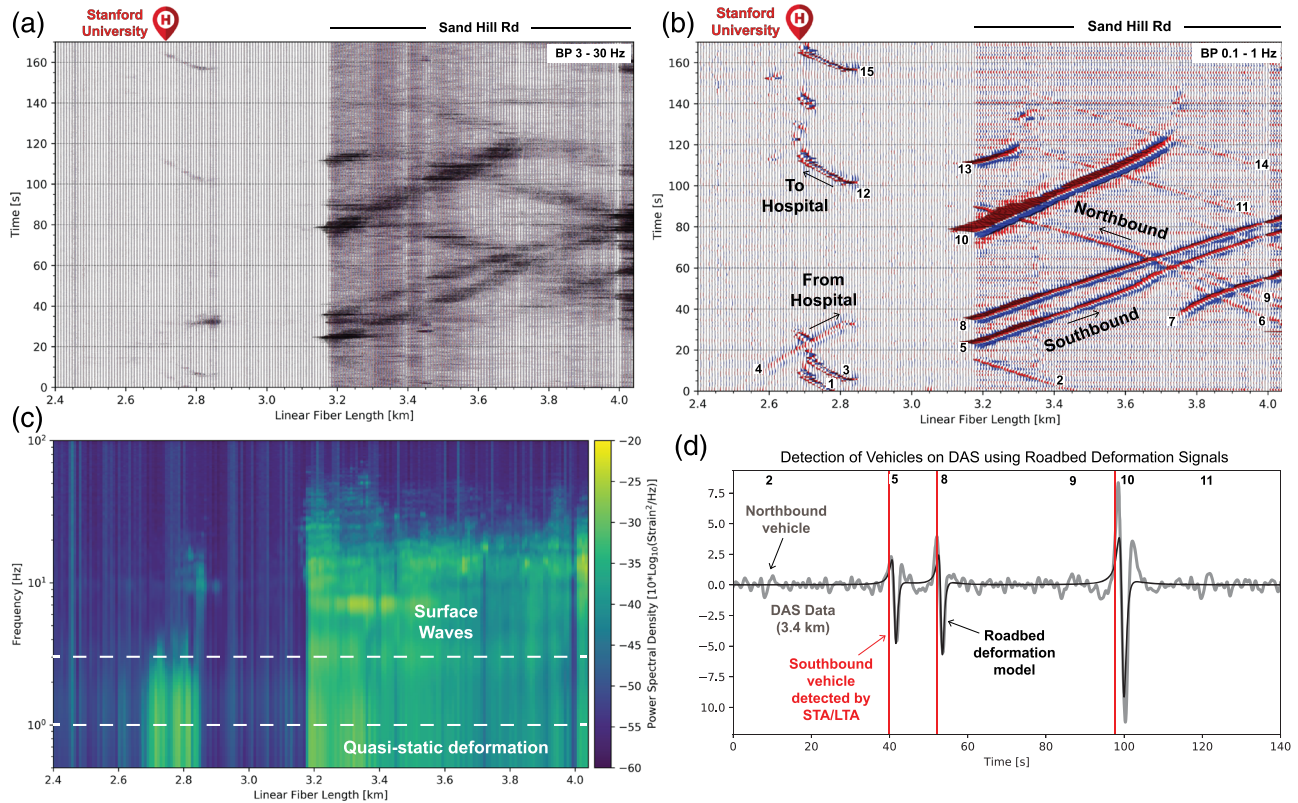
Figure 2. Vehicle observations from Stanford DAS-2 Experiment. (a) Example of DAS recordings bandpassed around 3–30 Hz showing vehicle surface waves and contrasting background energy between Stanford Hospital and Sand Hill Road sections. (b) Same as (a) but bandpassed around 0.1–1 Hz to highlight the high quality geodetic strain responses of the roadbed due to vehicle loading. Individual vehicles are numbered. (c) Continuous wavelet transform applied to spatial axis of unfiltered data shown in (a) and (b) highlighting dominant frequencies of different array segments. (d) Example processed strain data from DAS channel at 3.4 km, bandpass filtered as in (b) in gray, with a model of the horizontal strain for three vehicles passing the fiber on the southbound side of the road (black line), and three STA/LTA detections (red lines) for vehicles #5, #8, #10 shown in (b). A matched template algorithm was then applied using the median of approximately 200 detected vehicle signals and scanning over the full daily time series for the DAS channel.

figure are preprocessed strain time series recorded during a 3-min period from 10 March 2020 using the evenly spaced DAS array, and then bandpass filtered between 3 and 30 Hz. In this high frequency band, ground motion could be tracked coherently 100–200 m away from the vehicle, but longer wavelengths likely travel much further. The reduced seismic background at non-Sand Hill Road DAS channels was observed to transition sharply from high to low at $X = 3.18$ km where the fiber turned off of Sand Hill Road towards Stanford Hospital (see Figure 1a), potentially related to fiber directionality, distance from the road, and coupling.

Filtering the Palo Alto DAS data in a lower frequency range of 0.1–1 Hz revealed a localized wavelet pattern with peak amplitudes around 5–10 nanostrain, which migrate in time and space at the speed limit for the road (Figure 2b). Jousset et al. (2018) observed a similar low frequency horizontal strain response on optical fibers with a DAS experiment in Iceland and suggested it was related to the quasi-static or geodetic loading of passing vehicles.

In general, vehicular seismic sources can be modeled using a collection of vertical point forces located at the vehicle's wheel-road contacts (Ben-Zion & Zhu, 2002; Brenguier et al., 2019; Jousset et al., 2018; Li et al., 2018). The quasi-static or geodetic strain DAS signal from a vehicle is equal to the change in displacement over the DAS gauge length (L). Displacement in the direction of the fiber (u_x) can be modeled using the Flamant-Boussinesq equation for a point load applied to a half space with basic knowledge of the fiber and vehicle locations, the vehicle's mass, the soil shear modulus (μ), and Poisson's ratio (ν):
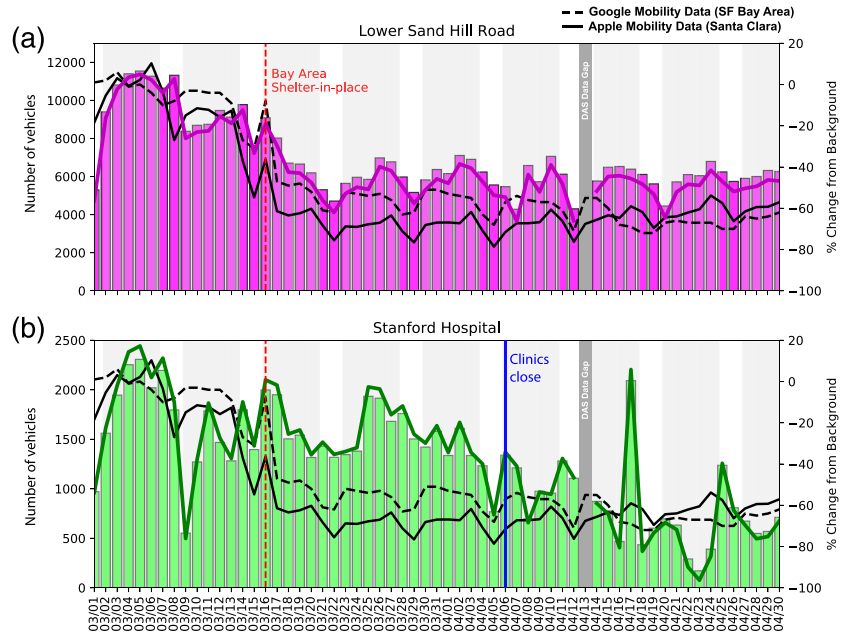
Figure 3. DAS vehicle detections measured before and during COVID-19 quarantine. (a) Number of vehicles (left y-axis) detected near Lower Sand Hill Road during morning commute between 4:00 am and 12:00 pm. Lines show the relative change as a percentage (right y-axis). Magenta line summarizes the change in DAS detections from a 7-day median background during the first week, compared with mobile phone statistics provided by Google (dashed black) and Apple (solid black). Vertical red and blue lines indicates timing of Bay Area shelter-in-place and date that some of the Stanford clinics closed near the fiber-optic array. Gray/white background represents weekdays/weekends. One data gap is shown when the DAS instrument was offline for maintenance. (b) Same as (a) for DAS channel near Stanford Hospital.

$$u_x(x) = \frac{F_z}{4\pi\mu}\left(\frac{zx}{r^3} - \frac{(1-2\nu)}{r+z}\left(\frac{x}{r}\right)\right), \tag{1}$$

$$\varepsilon_x = \frac{u\left(x+\frac{L}{2}\right) - u\left(x-\frac{L}{2}\right)}{L}. \tag{2}$$

In Equation 1, x represents fiber position, z is fiber depth, $r = \sqrt{x^2 + y^2 + z^2}$, and F_z is the weight of the vehicle. The measured horizontal displacement in the direction of the fiber (u_x) is linearly related to the vehicle's mass and falls off rapidly as $1/r^2$ as the fiber-vehicle distance increases, unlike higher frequency surface wave ground motions that radiate hundreds of meters beyond the vehicle's location. The shape of the horizontal strain response in x (ε_x) described in Equation 2, equivalent to the change in Equation 1 at two fiber positions separated by the gauge length, depends only on the vehicle's speed and Poisson's ratio. Strain amplitude scales with vehicle mass, but falls off like $1/r^2$ when the total strain response to a multiwheeled vehicle also depends on the interwheel separation or vehicle area. Based on a plausible parameter space, we determined that urban vehicles produce geodetic signals with energy around 0.1–1 Hz (see Text S1).

2.2. Vehicle Detection and Characterization

Vehicle-induced geodetic strains in the range 0.1–1 Hz were utilized in a template-matching algorithm to detect and characterize changes in Palo Alto vehicle traffic patterns during the COVID-19 quarantine (Figure 2d, see Text S1 for a description of the algorithm). Figure 3 shows the number of vehicles detected per day during the morning commute hours (4:00 am–12:00 pm) for two selected DAS locations marked in Figure 1. According to our results, the number of vehicles on Sand Hill Road decreased from about 11,000 per day to around 5,500 per day after the 16 March 2020 Bay Area shelter-in-place ordered. This is equal to a 40%–60% decrease in the measured number of vehicles relative to a background level which we
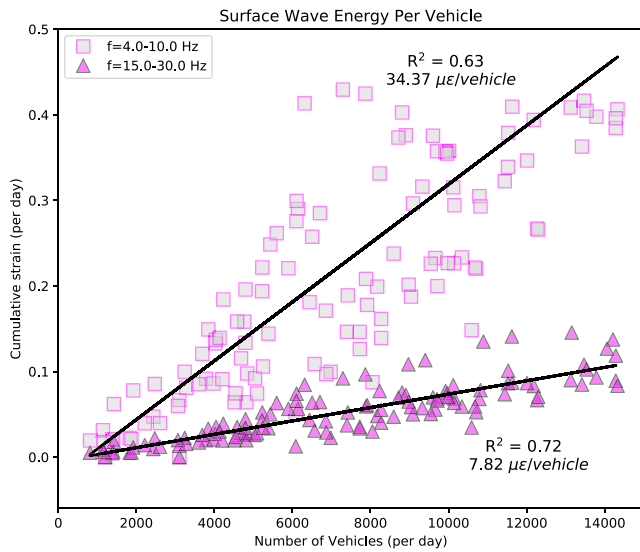
Figure 4. Relationship between anthropogenic surface waves and vehicle number. Total horizontal strain for the daytime hours recorded by a Lower Sand Hill Road DAS channel versus the number of vehicles detected by template matching. Two frequency bands are shown, $f = 4.0$–10.0 Hz (squares) and $f = 15.0$–30.0 Hz (triangles). The energy of surface waves produced by vehicles decays with decreasing wavelength and increasing propagation length; hence, the correlation improves at higher frequencies.

calculate from the median of the first week of the experiment (01 March 2020 through 07 March 2020, inclusive). Reduced traffic levels persisted through quarantine without increasing. Meanwhile, the number of vehicles detected using DAS data near Stanford Hospital documented a stable level of vehicles around 2,000 vehicles per day in the 2-week period after the order. Beginning around 06 April 2020, the vehicle activity near Stanford Hospital steadily declined to around 80% of the prequarantine level most likely as a result of the closure of the Stanford clinics (Rafiei, 2020), as well as Stanford Hospital instructing hospital staff to change where they parked their vehicles (Ho, 2020, personal communication). Additionally, the dramatic modification of traffic patterns in Palo Alto could have rerouted drivers to a faster route avoiding this part of the city. There were several anomalous times of vehicle activity such as on 17 April 2020 (Good Friday) and 25 April 2020 when it appears more vehicles were traveling in this area potentially to spend time outdoors on Stanford University's campus or surrounding parks. On 16 March 2020, the day of the shelter-in-place order, there is a single-day increase in traffic suggestive of people driving to the store to get supplies which is consistent with the reported 81% uptick in San Francisco Bay Area grocery store sales relative to March 2019 (Louie, 2020).

3. Discussion

One DAS experiment provides highly resolved statistics about public infrastructure utilization across many large sectors of a city through time. According to our results from the Stanford DAS-2 experiment, the COVID-19 quarantine order from local and state government officials resulted in a major decrease in commuter traffic along Sand Hill Road but sustained use of critical infrastructure such as the road near Stanford Hospital. The baseload of vehicle traffic on Sand Hill during the quarantine was likely related to essential business traffic like the major grocery store and pharmacies. These changes may seem obvious as Sand Hill is a commuter corridor connecting the I-280 freeway and CA-82 highway to businesses and workplaces that closed during quarantine while Stanford Hospital remained busy, but accurately quantifying these changes in real-time is a challenge.

A commonly reported metric during the quarantine was derived from mobile phone users. We find a strong correlation between the 50% decrease in vehicles counted using DAS on Sand Hill Road and the 50%–70% decrease in mobile phone-derived activity data reported by Apple (for Santa Clara County driving data) and by Google (for San Francisco Bay Area retail and recreation data; see Figure 3). Mobile phone data rely exclusively on a select pool of users, and thus will not include users making trips without data services, public transit vehicles, or police/fire/emergency vehicles, which were all still using Sand Hill Road during quarantine. Furthermore, the mobile phone data are aggregated for different regions, which may be less representative of Sand Hill Road. In comparison, a fiber-optic transportation sensing strategy yields an anonymous and absolute number of vehicles passing through a given sector.

Over 450,000 automatic vehicle detections were made using DAS on Sand Hill Road during the 8-week experiment. We found that the quasi-static or geodetic strain response to individual vehicle loading/unloading presented clear evidence of a proximate vehicle (Figure 2d). Because this strain falls off like $1/r^2$, vehicles passing far from the fiber such as on the opposite side of the street have a greater likelihood of being missed, as can be seen in Figure 2b where Northbound vehicles are weaker than Southbound ones (fiber is located on the Southbound side). While the template matching algorithm performs better than a simple threshold detection algorithm, more sophisticated methods that utilize machine learning or the distributed nature of DAS data are required to refine these results (Martin, 2018). The DAS-based transportation analysis is likely biased towards larger vehicles that create larger roadbed strains and also those vehicles traveling near the fiber. Extension of this algorithm to, for example, capture all vehicles on the

road with pristine accuracy, classify the vehicles in any way, or perform other tasks such as tracking pedestrians or bicyclists, which are already potentially tracked by mobile phone location services, is reserved for future work.

Spatially localized roadbed deformations from vehicles passing in the immediate vicinity of the fiber provide a more accurate detail about traffic patterns than is available to point sensor seismic measurements. This is because one urban seismometer, or more commonly a short geophone, only records high frequency anthropogenic surface waves. Such energy could be produced by vehicles traveling anywhere within a radius of several hundred meters. In Figure 4, we show that the DAS data from Sand Hill Road document a relationship between the number of vehicles and the total surface wave strain energy recorded in two different high frequency bands (4–10 Hz and 15–30 Hz). This relationship provides calibration of the vehicle component of the anthropogenic surface wave background recorded by seismometers.

In times of crisis, access to DAS-derived information about public infrastructure utilization is valuable to public health and government officials because it provides city-wide measurements which are natively anonymized and aggregated with the requisite level of spatial and temporal granularity to make decisions. DAS retrieves data about how infrastructure is being used across a large urban area with an easily deployable instrument.

Funding Information

Conflict of Interest

There are no competing interests.

Data Availability Statement

Data used to support the conclusions of this article are available at https://purl.stanford.edu/bt630qc9349.

References

Ajo-Franklin, J. B., Dou, S., Lindsey, N. J., Monga, I., Tracy, C., Robertson, M., et al. (2019). Distributed acoustic sensing using dark fiber for near-surface characterization and broadband seismic event detection. *Scientific Reports*, *9*(1), 1–14.

Apple (2020). Mobility Trends Reports. Available at: https://www.apple.com/covid19/mobility (accessed: 25 April 2020).

Ben-Zion, Y., & Zhu, L. (2002). Potency-magnitude scaling relations for southern California earthquakes with 1.0< M L< 7.0. *Geophysical Journal International*, *148*(3), F1–F5. https://doi.org/10.1046/j.1365-246X.2002.01637.x

Brenguier, F., Boué, P., Ben-Zion, Y., Vernon, F., Johnson, C. W., Mordret, A., et al. (2019). Train traffic as a powerful noise source for monitoring active faults with seismic interferometry. *Geophysical Research Letters*, *46*, 9529–9536. https://doi.org/10.1029/2019GL083438

Coward, D., Turner, J., Blair, D., & Galybin, K. (2005). Characterizing seismic noise in the 2–20 Hz band at a gravitational wave observatory. *Review of scientific instruments*, *76*(4), 044501.

Díaz, J., Ruiz, M., Sánchez-Pastor, P. S., & Romero, P. (2017). Urban seismology: On the origin of earth vibrations within a city. *Scientific Reports*, *7*(1), 1–11.

Dou, S., Lindsey, N., Wagner, A. M., Daley, T. M., Freifeld, B., Robertson, M., et al. (2017). Distributed acoustic sensing for seismic monitoring of the near surface: A traffic-noise interferometry case study. *Scientific Reports*, *7*(1), 1–12.

Fang, G., Li, Y. E., Zhao, Y., & Martin, E. R. (2020). Urban near-surface seismic monitoring using distributed acoustic sensing. *Geophysical Research Letters*, *47*, e2019GL086115. https://doi.org/10.1029/2019GL086115

Ferguson, N., Laydon, D., Nedjati Gilani, G., Imai, N., Ainslie, K., Baguelin, M., et al. (2020). Report 9: Impact of non-pharmaceutical interventions (NPIs) to reduce COVID19 mortality and healthcare demand.

Google (2020). COVID-19 Community Mobility Reports. Available at: https://www.google.com/covid19/mobility/ (accessed: 25 April 2020).

Ho, F. (2020). Text message to Nate Lindsey, May 4.

Inbal, A., Clayton, R. W., & Ampuero, J. P. (2015). Imaging widespread seismicity at midlower crustal depths beneath Long Beach, CA, with a dense seismic array: Evidence for a depth-dependent earthquake size distribution. *Geophysical Research Letters*, *42*, 6314–6323. https://doi.org/10.1002/2015GL064942

Jousset, P., Reinsch, T., Ryberg, T., Blanck, H., Clarke, A., Aghayev, R., et al. (2018). Dynamic strain determination using fibre-optic cables allows imaging of seismological and structural features. *Nature Communications*, *9*(1), 1–11.

Krischer, L., Megies, T., Barsch, R., Beyreuther, M., Lecocq, T., Caudron, C., & Wassermann, J. (2015). ObsPy: A bridge for seismology into the scientific Python ecosystem. *Computational Science & Discovery*, *8*(1), 014003.

Lecocq, T. (2020). SeismoRMS, Github repository, https://github.com/ThomasLecocq/SeismoRMS (Accessed April 1, 2020).

Lecocq, T., Hicks, S. P., Van Noten, K., van Wijk, K., Koelemeijer, P., De Plaen, S. M., et al. (2020). Global quieting of high-frequency seismic noise due to COVID-19 pandemic lockdown measures *Science*. https://doi.org/10.1126/science.abd2438

Li, L., Nimbalkar, S., & Zhong, R. (2018). Finite element model of ballasted railway with infinite boundaries considering effects of moving train loads and Rayleigh waves. *Soil Dynamics and Earthquake Engineering*, *114*, 147–153. https://doi.org/10.1016/j.soildyn.2018.06.033

Lindsey, N. J., Martin, E. R., Dreger, D. S., Freifeld, B., Cole, S., James, S. R., et al. (2017). Fiber-optic network observations of earthquake wavefields. *Geophysical Research Letters*, *44*, 11,792–11,799. https://doi.org/10.1002/2017GL075722

Louie, D. (2020). 'Coronavirus: Research shows big changes in Bay Area spending habits during COVID-19 shelter-in-place', *ABC-7 Bay Area News*, 1 May. Website: https://abc7news.com/bay-area-coronavirus-update-california-shelter-in-place-lockdown/6144221/. Accessed July 15, 2020.

Martin, E. R. (2018). *Passive Imaging and Characterization of the Subsurface with Distributed Acoustic Sensing*, Stanford, CA: Doctoral dissertation, Stanford University.

Martin, E. R., Biondi, B. L., Karrenbach, M., & Cole, S. (2017). Continuous subsurface monitoring by passive seismic with distributed acoustic sensors-the "Stanford Array" experiment. In *First EAGE Workshop on Practical Reservoir Monitoring (Cp-505-00018)*, Amsterdam, The Netherlands: European Association of Geoscientists & Engineers.

Martins, H. F., Fernández-Ruiz, M. R., Costa, L., Williams, E., Zhan, Z., Martin-Lopez, S., & Gonzalez-Herraez, M. (2019, March). Monitoring of remote seismic events in metropolitan area fibers using distributed acoustic sensing (DAS) and spatio-temporal signal processing. In *2019 Optical Fiber Communications Conference and Exhibition (OFC)* (pp. 1–3). San Diego, CA: IEEE.

Masoudi, A., & Newson, T. P. (2016). Contributed review: Distributed optical fibre dynamic strain sensing. *Review of scientific instruments*, *87*(1), 011501.

Meremonte, M., Frankel, A., Cranswick, E., Carver, D., & Worley, D. (1996). Urban seismology—Northridge aftershocks recorded by multi-scale arrays of portable digital seismographs. *Bulletin of the Seismological Society of America*, *86*(5), 1350–1363.

Nakamura, Y. (1989). A method for dynamic characteristics estimation of subsurface using microtremor on the ground surface. *Railway Technical Research Institute, Quarterly Reports*, *30*(1).

Oliver, N., Lepri, B., Sterly, H., Lambiotte, R., Deletaille, S., De Nadai, M., et al. (2020). Mobile phone data for informing public health actions across the COVID-19 pandemic life cycle. *Science Advances*, *6*(23), eabc0764. https://doi.org/10.1126/sciadv.abc0764

Poli, P., Boaga, J., Molinari, I., Cascone, V., & Boschi, L. (2020). The 2020 coronavirus lockdown and seismic monitoring of anthropic activities in Northern Italy. *Scientific Reports*, *10*, 9404. https://doi.org/10.1038/s41598-020-66368-0

Posey, R. (2000, November). Rayleigh scattering based distributed sensing system for structural monitoring. In *Fourteenth International Conference on Optical Fiber Sensors* (Vol. 4185, 41850E). Venice, Italy: International Society for Optics and Photonics.

Rafiei, Y. (2020). Stanford's safety-net clinics closed in response to coronavirus, *The Stanford Daily*, 7 April. Website: https://www.stanforddaily.com/2020/04/07/stanfords-safety-net-clinics-closed-in-response-to-coronavirus/. Accessed July 15, 2020.

Spica, Z. J., Perton, M., Martin, E. R., Beroza, G. C., & Biondi, B. (2020). Urban Seismic Site Characterization by Fiber-Optic Seismology. *Journal of Geophysical Research: Solid Earth*, *125*, e2019JB018865. https://doi.org/10.1029/2019JB018656

Tian, H., Liu, Y., Li, Y., Wu, C. H., Chen, B., Kraemer, M. U., et al. (2020). An investigation of transmission control measures during the first 50 days of the COVID-19 epidemic in China. *Science*, *368*(6491), 638–642. https://doi.org/10.1126/science.abb6105

Tizzoni, M., Bajardi, P., Decuyper, A., King, G. K. K., Schneider, C. M., Blondel, V., et al. (2014). On the use of human mobility proxies for modeling epidemics. *PLoS Computational Biology*, *10*(7), e1003716. https://doi.org/10.1371/journal.pcbi.1003716

Vidale, J. E. (2011). Seattle "12th man earthquake" goes viral. *Seismological Research Letters*, *82*(3), 449–450. https://doi.org/10.1785/gssrl.82.3.449

Wellbrock, G. A., Xia, T. J., Huang, M. F., Chen, Y., Salemi, M., Huang, Y. K., et al. (2019). First field trial of sensing vehicle speed, density, and road conditions by using fiber carrying high speed data. In *2019 Optical Fiber Communications Conference and Exhibition (OFC)* (pp. 1–3). San Diego, CA: IEEE.

Wesolowski, A., Eagle, N., Noor, A. M., Snow, R. W., & Buckee, C. O. (2013). The impact of biases in mobile phone ownership on estimates of human mobility. *Journal of the Royal Society Interface*, *10*(81), 20120986.

Wesolowski, A., Eagle, N., Tatem, A. J., Smith, D. L., Noor, A. M., Snow, R. W., & Buckee, C. O. (2012). Quantifying the impact of human mobility on malaria. *Science*, *338*(6104), 267–270. https://doi.org/10.1126/science.1223467

Xiao, H., Eilon, Z., Ji, C. & Tanimoto, T. (2020). COVID-19 Societal Response Captured by Seismic Noise in China and Italy, *Seismological Research Letters*. https://doi.org/10.1785/0220200147

References From the Supporting Information

Yuan, S., Lellouch, A., Clapp, R. G. & Biondi, B. (2020). Near-surface characterization using a roadside distributed acoustic sensing Array. *arXiv preprint arXiv:2006.01360*.